

CHEMICAL CHARACTERISTICS OF THE SOOT PRODUCED IN A HIGH-SPEED DIRECT INJECTION ENGINE OPERATED WITH DIESEL/BIODIESEL BLENDS

Maurin Salamanca,¹ John R. Agudelo,² Fanor Mondragón,¹ and Alexander Santamaría¹

¹Energy Resources and Environmental Chemistry Group (QUIREMA), Institute of Chemistry, University of Antioquia, Medellín, Colombia

²Group of Efficient Energy Management (GIMEL), Faculty of Engineering, University of Antioquia, Medellín, Colombia

The aim of this work is to study the influence of the molecular structure of fatty acid esters present in biodiesel and their blends with diesel on the chemical characteristics of the emitted particulate matter. Biodiesel produced from palm oil, jatropha, castor oil and sachainchi was blended at 5% and 20% by volume with diesel. These fuels were used for the operation of a four-cylinder direct injection automotive diesel engine. The equivalent ratio was kept between 0.36 and 0.40, and the engine was operated at the point of minimum air–fuel ratio and maximum smoke opacity. The amount of particulate matter emitted was evaluated by opacity index. A marked reduction in soot formation was observed when the concentration of unsaturated methyl esters in the fuel was at low concentrations. This was accompanied by a reduction of the aliphatic carbon content in the particulate matter.

Keywords: Biodiesel; Chemical characterization; Chemical structure; Direct injection engine; Particulate matter

INTRODUCTION

Fossil fuels will remain as the main energy source for transportation for many years, even though it is well known that they cause a severe impact on the environment. Therefore several alternatives have been investigated to substitute them (Abbasi and Abassi, 2010). The most promising options are the renewable fuels, such as biodiesel and bioethanol (Kohse-Höinghaus et al., 2010). Biodiesel production and performance in engines have been investigated the last few decades. General trends of the impact of biodiesel on engine emissions have been published. However,

Received 8 July 2011; revised 6 December 2011; accepted 1 February 2012.

Published as part of the Seventh Mediterranean Combustion Symposium Special Issue with Guest Editors Federico Beretta, Nevin Selçuk, Mohy S. Mansour, and Andrea D'Anna.

Address correspondence to Alexander Santamaría, Energy Resources and Environmental Chemistry Group (QUIREMA), Institute of Chemistry, University of Antioquia, Carrera 53 No 61-30, Medellín, A.A. 1226, Colombia. E-mail: alex.santamar@matematicas.udea.edu.co; alex.santamar@gmail.com

that information depends on the engine type, operating conditions, and the chemical nature of the biodiesel used (Szybist et al., 2007).

The use of biodiesel in internal combustion engines usually increases the amount of nitrogen oxides produced. Zhu et al. (2010) used rapeseed methyl ester (RME) and palm methyl ester (PME) in a Cummins 4BTA direct injection diesel engine. They found that PME blends give higher NO_x emissions than RME blends due to the higher viscosity and oxygen content of PME compared with RME.

A relationship between the amount of biodiesel in a blend with diesel and the reduction of particulate matter emitted has been previously established (Lapuerta et al., 2008). This reduction is related to the oxygen present in the chemical structure of the biodiesel and the existence or nonexistence of highly diluted aromatic compounds in the final fuel. Zhang et al. (2011) found a significant reduction of particulate matter and total hydrocarbons by using a four-cylinder direct injection diesel engine operated with soybean oil and waste cooking oil. They also quantified the amount of organic carbon (OC) and elemental carbon (EC) in particulate matter and found that the ratio between these two parameters depends on the type of fuel and the operation condition.

Lapuerta et al. (2005), using sunflower methyl ester (SME) and cynara cardunculus methyl ester (CME) in a diesel engine operated at five different conditions, found that the amount of soot collected on filters strongly decreased as the concentration of biodiesel increased. For the soluble organic fraction (SOF), they did not find significant differences, since not all of the adsorbed hydrocarbons come from fuel, so that, the major contribution to SOF came from lube oil in these test conditions.

An approach for understanding how biofuels can change particle size distribution and concentration was made by Maricq (2011) using a diffusion flame of methyl butanoate as biodiesel surrogate and soy fatty acid methyl esters (FAME). The value of the first and second modes for particle size distribution decreases slightly when the measurement is done with soy oil. A higher soot reduction was found when methyl butanoate was used. In all cases C_xH_y ions, PAH ions, and fullerene ions were observed in the mass spectra. Also, the mole fraction of each of these compounds was a function of the chemical nature of the fuel.

The purpose of this work is to evaluate variations in the soot chemical composition induced by addition of biodiesel to a diesel No. 2 using a high-speed, direct-injection diesel engine under a maximum opacity condition.

EXPERIMENTAL SETUP

Engine Test and Sampling Procedure

Tests were carried out in an instrumented automotive diesel engine (Table 1). The engine was operated at 2450 rpm and 95 Nm. These conditions were chosen because it was the point of minimum air–fuel ratio and maximum smoke opacity according to the FTP75 homologation cycle, which was obtained via vehicle dynamics analysis. When this type of engine is used in a vehicle driven during this cycle, the engine speed and torque are in the range between 1600 rpm and 30 Nm and 2750 rpm and 98 Nm, corresponding to approximately 80% of the area used by the engine during the homologation cycle and/or during real driving conditions.

Table 1 Diesel engine characteristics

Parameter	Value
Reference	ISUZU 4JA1
Type	Turbocharged, direct injection, rotating pump
Swept volume	2499 cm ³
Configuration	4 in-line cylinders
Diameter × stroke	93 mm × 92 mm
Compression ratio	18.4
Rated power	59 kW (80 hp) at 4100 rpm
Maximum torque	98 Nm at 2750 rpm

The tests were performed with diesel blended at 5% and 20% with each of the following biodiesels: palm (BP), sachu inchi (BS), jatropha (BJ), and castor oil (BC); additionally, blends at 50% and 100% of palm biodiesel were studied. Commercial grade No.2 diesel was used as the reference fuel. The diesel No. 2 had an elemental composition by weight of 87.2% carbon, 12.8% hydrogen, and 0.0225% sulfur, and an aromatic content of 29.3% (13% monoaromatics, 13.3% diaromatics, and 3% polyaromatics). The main components of the different oils used on this work are presented in Table 2.

After each fuel was tested, fuel pipes were drained prior to the following experiment. The engine was operated for at least 1 h with the new fuel to purge any of the remaining non-test fuel in the engine. Measurements were carried out for 5 h (for each fuel) of continuous stationary operation in order to guarantee enough particle matter for the chemical and morphological analysis (30–50 mg). Tests with different fuels were carried out without any modification on the engine or its fuel injection system. The test unit was located at 1500 m above sea level.

The soot samples were taken at the exhaust pipe using a 50-cm-length stainless steel probe, which was connected to a vacuum system in line with a Teflon filter of 0.25- μ m pore diameter that was used to collect the particulate matter (PM) and low molecular-weight compounds that condense at 40°C. A cold trap was also used to capture water and condensable compounds that passed through the filter.

Table 2 Biodiesel composition, and in parenthesis, the number of carbon atoms followed by the number of double bonds of the main fatty acid

Fatty Acids	Biodiesel			
	BP (%)	BJ (%)	BC (%)	BS (%)
Palmitic (16:0)	43.5	14.4	1.8	4.6
Oleic (18:1)	41.0	34.4	4.7	8.2
Linoleic (18:2)	9.4	44.1	5.7	27.5
Linolenic (18:3)	0.2	–	0.5	55.7
Stearic (18:0)	4.3	6.1	1.1	2.1
Ricinoleic (18:1)	–	–	86.2	–
Others	1.6	1.0	0.0	2.1

Soot Chemical Characterization

Thermogravimetric analysis (TGA) of soot collected in the filters located at the engine exhaust was carried out at 800°C under nitrogen atmosphere to determine water and the volatile fraction in the PM. Once the temperature reached 800°C, the sample was iso-thermally hold during 12 min in nitrogen and then oxidized in air to get the combustion of the fixed carbon content in the sample, which is sometimes associated with the elemental carbon. All experiments were carried in a TA Instruments 2950 unit and the total flow rate of gases was adjusted at 100 mL/min during each test.

For qualitative Fourier transformed-infrared spectroscopy (FT-IR) analysis, a small amount of soot collected on a filter was used to prepare a 1% KBr pellet. Each spectrum was the result of 300 scan accumulation, a value that provided the best signal/noise ratio. A Nicolet Magna 560 spectrometer was used with a MCT/A detector.

Raman spectra of the PM samples were recorded with a Raman microscope system (lab Raman HR Horiba) using a 632.8 nm laser line as an excitation source. Spectra of the samples were in the range of 100–3600 cm^{-1} with a 50 × magnification objective and 20 s exposition time. The spectra were processed with the free software Lab Plot. After a multipoint baseline correction, spectra were fitted by a combination of three Lorentzian curves to characterize the G (graphitic) and D (non-graphitic) bands at about 1550 and 1350 cm^{-1} , respectively.

Identification and semi-quantitative analysis of elements present on the airborne particles that were collected on the filters were performed in an EDX Oxford Instruments Inca Penta Fetx3 unit operated at an excitation voltage of 50 kV during a collection time of 30 s. Also, elemental analysis composition was determined by X-ray fluorescence spectroscopy using a Thermo Scientific ARL Optim'x equipment.

Size and morphology of the PM were carried out by transmission electron microscopy (TEM). In this study, a small amount of PM was deposited on the formvar grid and then placed on a JEOL JEM 1200 EX microscope operated at a voltage range between 20 to 120 kV. Measurement of the particle size was done manually on the micrographs using the free ImageJ software, taken at a 100 nm scale as a reference marker.

RESULTS

Engine Performance

Table 3 shows the engine performance results comparing biodiesel fuels with diesel No. 2 fuel. Each result is the average of five measurements (one per hour of test). The break power used in the engine was almost the same for all fuels, which guarantees that measurements were carried out under the same energy output. The equivalence ratio was similar for all fuels, indicating that the differences in performance and emissions were not affected by this parameter, but by differences in biodiesel composition and properties. It was also found that the smoke opacity, a property related with the particulate matter emission, was higher for diesel compared to biodiesel fuels. However, this property increased among the biodiesel fuels according to the degree of unsaturation.

Based on the opacity index reported in Table 3, it can be inferred that, in general, the amount of particulate matter emission decreases as biodiesel content

Table 3 Engine performance with diesel and biodiesel blends

Fuel	Brake power (kW)	Equivalence ratio	In-cylinder Tmax (°C)	Opacity (%)
Diesel	24.0	0.37	1674	1.9
BP5	23.8	0.36	1653	1.9
BP20	23.8	0.38	1698	1.0
BP100	23.9	0.37	1710	0.6
BJ5	23.9	0.38	1652	1.5
BJ20	24.4	0.39	1643	1.3
BC5	24.0	0.39	1660	1.5
BC20	23.7	0.40	1695	1.2
BS5	24.1	0.38	–	1.9
BS20	23.9	0.37	–	2.0

increases. This reduction was clearly evident in the diesel/biodiesel blends of 5%, 20%, and 100% palm and castor oil. In the case of 100% palm biodiesel, a reduction of 65% in the opacity index was observed compared to the opacity index of the reference fuel. This result is due to an increase in the oxygen fuel content and the absence of aromatic and unsaturated hydrocarbons compounds on biodiesels, promoting the reduction of soot and soot precursors. The only biodiesel that did not show this trend was *sacha inchi*, since the opacity index remained almost constant, independent of the amount of biodiesel used. In order to give an explanation of the behavior described above, several studies have pointed out that a correlation between the chemical structure of the biodiesel components and the tendency to produce PM can exist (Glassman, 1996; Zhang et al., 2008). Table 4 shows the chemical structure of the major components (methyl esters) present in the various biodiesel used in this study.

Based on the chemical structure of methylesters present in the biodiesels evaluated here, it can be seen that the fuel with a high content of methyl linolenate, *sacha inchi*, has a low tendency to reduce the amount of particulate matter due in part to the presence of three consecutive double bonds units structure, which in turn can favor the formation of soot precursors. On the other hand, castor oil biodiesel, consisting mainly of methyl ricinoleate with an OH group in its structure, facilitates the oxidation process that eventually will be reflected in the reduction of particulate matter as well as in the opacity index.

Soot Particle Characterization

Table 5 summarizes the results obtained by thermogravimetric analysis of the PM of different biodiesels used in this study. In general, an increment in the fixed carbon content was observed in most of the PM samples coming from biodiesel or their blends compared to PM of diesel, followed by a decrease in the volatile matter as the amount of biodiesel added to the fuel increases, as was observed for the palm biodiesel series.

On the other hand, most of PM samples showed a reduction in the ash content compared to diesel, except for BP 100 a behavior that can be explained by the

Table 4 Chemical structure of the major components present in biodiesel

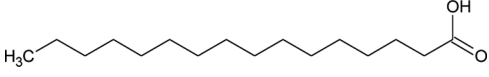
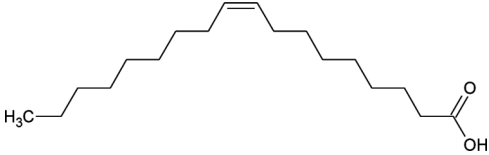
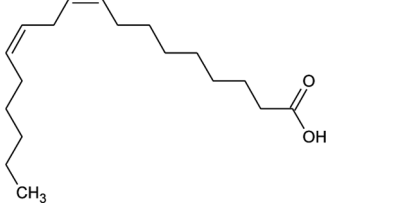
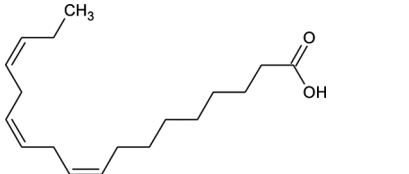
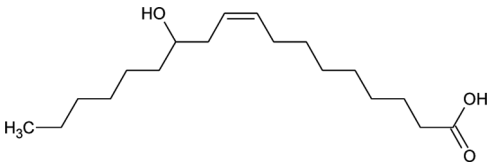
Molecular formula	Chemical structure
Palmitic acid $C_{16}H_{32}O_2$	
Oleic acid $C_{18}H_{34}O_2$	
Linoleic acid $C_{18}H_{32}O_2$	
Linolenic acid $C_{18}H_{30}O_2$	
Ricinoleic acid $C_{18}H_{34}O_3$	

Table 5 Proximate analysis of soot samples

Fuel	Volatile matter (%) 120–800°C	Fixed carbon (%) comb. 800°C	Residue (%)
Diesel	50.9	40.2	8.9
BP5	47.1	45.8	7.1
BP20	45.4	48.2	6.4
BP50	46.7	46.4	6.8
BP100	46.7	41.6	11.7
BH5	44.0	48.2	7.8
BH20	49.2	45.8	5.0
BJ5	43.3	51.6	5.2
BJ20	46.5	47.2	6.4
BS5	47.8	44.8	7.3
BS20	43.7	49.1	7.2

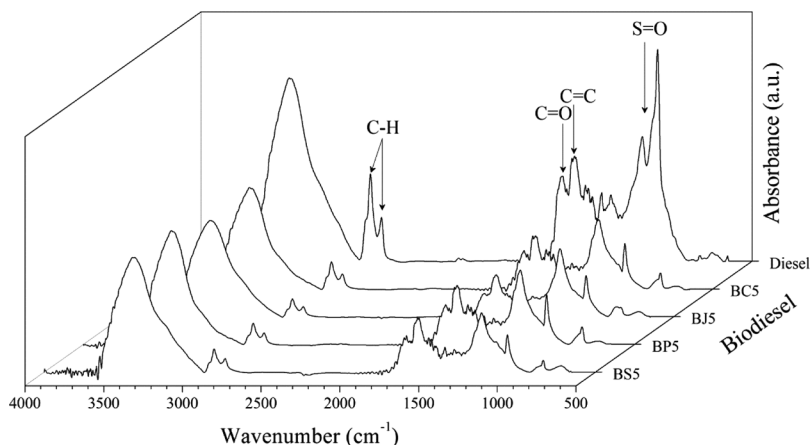


Figure 1 Infrared spectra of PM coming from diesel and 5% biodiesel blended with diesel.

increase of the oxygen content into the fuel, which promotes a change in the mass basis of calculation due to the removal of carbon from particle phase caused by oxidation.

Figure 1 shows the infrared spectra of particulate matter samples generated in the engine. It is observed that the most characteristic signals of soot coincide with those reported by Santamaría et al. (2006) and Cain et al. (2010); also, there are some peaks related to sulfur species, between 1000–1300 cm^{-1} . The wavenumber and the assignation of each peak are listed in Table 6.

In Figure 1, it is seen that the aromatic C-H signal is missing—a fact that could be related with the type of aromatic compounds. The larger the aromatic cluster the lower the hydrogen content becomes, indicating that the aromatic C-H vibrations are less intense or in some cases undetected by FT-IR. The addition of biodiesel also caused a reduction in the aliphatic character of the samples, even for the lowest biodiesel content.

Figure 2 shows the infrared spectra of PM as a function of palm-biodiesel concentration. The intensities of the most prominent signals are reduced to about half of the initial value, due to biodiesel addition, especially the signals corresponding to aliphatic and sulfate-like species. It is believed that this reduction is promoted by fuel dilution and an increased in the fuel oxygen caused by biodiesel addition, which

Table 6 FT-IR peaks assignment for soot samples

Absorption peak (cm^{-1})	Assignments
2975–2925–2850	Asymmetric and symmetric CH stretching of aliphatic groups
1715	C=O Carbonyl stretching
1610	C=C Aromatic and alkenes stretching
1450–1380	Asymmetric CH_3 and scissor CH_2 deformations Symmetric CH_3 deformation and cyclic CH_2
1290–1050	S=O Sulfate asymmetric and symmetric stretching

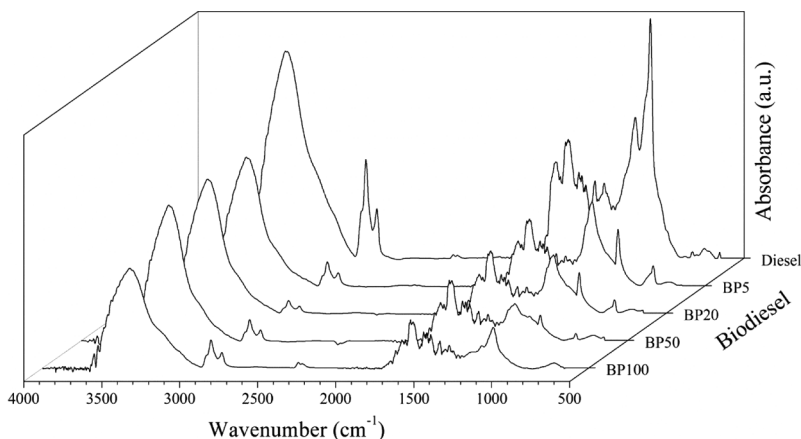


Figure 2 Infrared spectra of PM as a function of palm biodiesel concentration.

facilitates the oxidation processes. Although BP100 does not contain sulfur in its composition, the S=O signal remaining in the spectrum corresponds to the sulfur that comes from the lubricant oil.

Table 7 shows the elemental composition of particulate matter obtained by energy dispersive X-ray (EDX) spectroscopy and X-ray fluorescence (XRF). The composition does not include hydrogen, since it is an element that cannot be determined by these techniques. Also, elements below 2% can be analyzed qualitatively but cannot be quantified by EDX; due to this, some trace elements were quantified by XFR and labeled in Table 6 with an asterisk.

In general, the elemental analysis obtained by EDX and XRF indicates that most of PM samples from diesel/biodiesel blends have an average value of 73.5% for carbon, 21.2% for oxygen, and between 4–6.5% for sulfur. Besides the aforementioned elements, the samples also contain zinc, calcium, copper, and sodium, among others. Additionally, it is observed in Table 6 that BP5, BP20, BP50, and BP100 show a decrease in the amount of sulfur, being more significant for BP100. This result is expected since biodiesel does not contain sulfur in its composition, so that its content decreases as fuel dilution increases by biodiesel addition.

Table 7 Composition of particle matter from biodiesel blends by EDX and XRF

Fuel	Elements						
	C	O	S	Zn($\times 10^3$)	Ca($\times 10^2$)	Si($\times 10^2$)	Fe($\times 10^2$)
Diesel	76 \pm 4	19 \pm 5	3.6 \pm 0.1*	46 \pm 2*	14 \pm 1*	29 \pm 3*	6.8 \pm 1*
BP5	69 \pm 3	23 \pm 5	6.8 \pm 0.1*	65 \pm 3*	19 \pm 1*	25 \pm 2*	8.5 \pm 1*
BP20	70 \pm 3	23 \pm 3	6.7 \pm 0.1*	78 \pm 4*	10 \pm 1*	18 \pm 2*	14 \pm 1*
BP50	74 \pm 2	21 \pm 1	4.1 \pm 0.1*	61 \pm 3*	16 \pm 1*	32 \pm 4*	19 \pm 1*
BP100	80 \pm 3	19 \pm 4	0.64 \pm 0.04*	26 \pm 1*	12 \pm 1*	26 \pm 2*	7 \pm 1*
BS5	71 \pm 2	24 \pm 3	4 \pm 1	0.6 \pm 0.3	–	–	–
BS20	77 \pm 2	19 \pm 3	3 \pm 2	0.8 \pm 0.4	0.2 \pm 0.1	–	–

*Values obtained for XRF data.

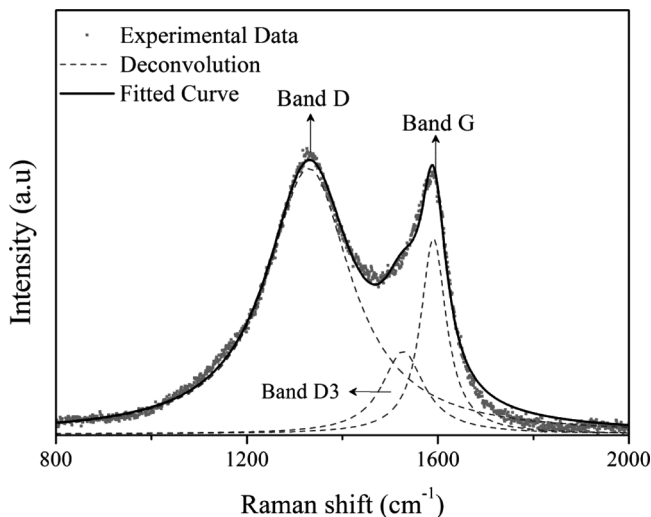


Figure 3 Raman spectra of a typical soot samples with palm biodiesel.

Some authors have reported that others elements besides C, H, and O may arise from the unwanted combustion of lubricants and their additives (e.g., Zn). The source of other elements (e.g., Si) may be from in organic components or organic complexes present in biomass, these elements can be converted into aerosols during the combustion processes. Alkali (e.g., Na) and alkaline earth (Ca) elements can come from the transesterification process (Aggadi et al., 2006; Schönborn et al., 2009; Vander Wal et al., 2010).

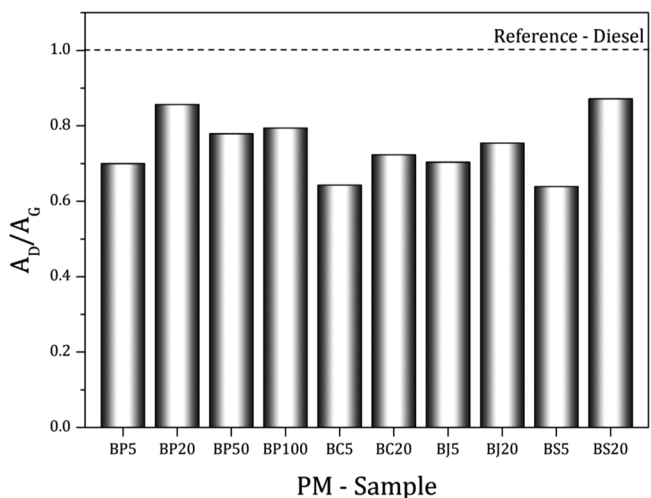


Figure 4 Ratio of graphitic and defect regions, AD/AG, of the particulate matter samples produced in the combustion of diesel and diesel/biodiesel blends.

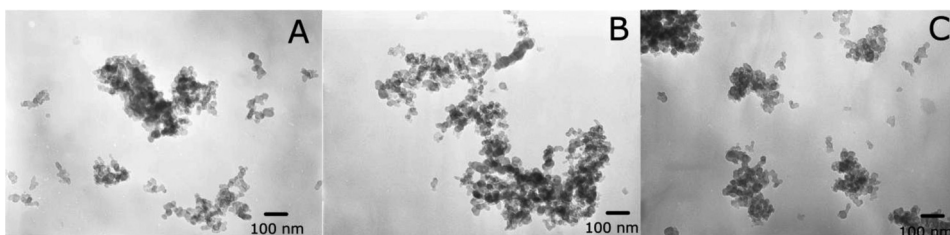


Figure 5 TEM images of PM obtained from (A) diesel, (B) BC5, and (C) BC20.

The Raman spectrum deconvolution was carried with three Lorentzian functions, for the G band associated with organized graphitic carbon, the D band related to defects on graphitic layers, and the D3 band related to sp^3 carbon configuration (Song et al., 2006). The deconvolution and fitting curves are shown in Figure 3. The A_D/A_G ratio was calculated for each Raman spectrum, based on area values, and the results are shown in the Figure 4. It is observed that the graphitic carbon content increases as biodiesel content increases, leading to a reduction in the A_D/A_G ratio, which is a result that agrees with the TGA data.

Other studies have established that biodiesel can have a different graphitization degree depending on combustion conditions such as thermal evolution in the combustion chamber, exhaust gas recirculation, and the chemical characteristics of the initial fuel (Al-Qurashi and Boehman, 2008; Song et al., 2006).

The morphological analysis obtained by TEM offers information about the size and degree of crystallinity of the particulate matter taken at the exhaust of the engine. Figure 5 shows the micrographs obtained for some samples. The samples

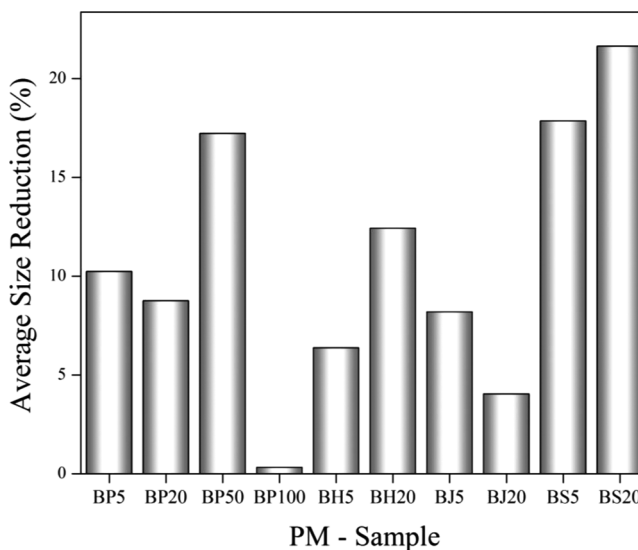


Figure 6 Average particle size reduction of PM coming from biodiesel.

have the typical chain-like structure composed of primary particles, with average size of 20.0 nm.

Figure 6 indicates that the average particle size can reach up to 21% reduction compared to diesel when BS20 is used. Similarly, most of the biodiesels evaluated in this study generated a particulate matter of smaller size than that of pure diesel a result that can be associated with an increase in the oxidation process caused by the presence of biodiesel, since it is through that the nonmolecular oxygen coming from biodiesel is more active than the molecular oxygen itself. However, further investigation needs to be addressed to get a reliable explanation. It is important to notice that that BP100 produces less soot emission, and its particle size remained constant compared to diesel. We believe that this behavior is related with the increase in the ash content that can promote nucleation and particle size growth during the pyrolysis process.

CONCLUSIONS

Biodiesel addition to diesel generates a significant reduction on the amount of particulate matter emitted when concentration of unsaturated methyl esters, such as methyl linolenate, is low. Also it was seen that the higher the biodiesel content, the higher the reduction of particulate matter.

Although the quality of biodiesel is not the same in every place of the world, the major components of each type of biodiesel will remain the same. These characteristics will determine the nature of particulate matter emitted as it was evaluated in this study.

The effect of biodiesel addition on the chemical characteristics of particulate matter was reflected in the reduction of carbon as well as the aliphatic character of the soot accompanied by an increment of the fixed carbon content, a result that correlates with the graphitic organization observed by Raman and the increase in the C=C stretching mode observed by FT-IR. A slight decrease in particle size was also observed when biodiesel was added to the fuel. Oxygen incorporation and sulfur reduction in the particulate matter was confirmed as one of the characteristics of the effect of the addition of biodiesel to fossil diesel.

ACKNOWLEDGMENTS

The authors want to thank the Colombian Ministry of Agriculture and Rural Development and the Environmental authority from Medellín (Área Metropolitana del Valle de Aburrá) for the financial support of project No. 003 2007D3608-67-07 (Biodiesel project). The authors also would like to thank the Sostenibilidad Program 2012–2013 of the University of Antioquia for financial support. M.S. thanks COLCIENCIAS and the University of Antioquia for the Ph.D. scholarship.

REFERENCES

- Abbasi, T., and Abassi, A.S. 2010. Biomass energy and the environmental impacts associated with its production and utilization. *Renewable Sustainable Energy Rev.*, **14**, 919.

- Aggadi, N., Arnas, C., Bénédicta, F., Dominique, C., Duten, X., Silva, F., Hassouni, K., and Gruen, D.M. 2006. Structural and chemical characterisation of soot particles formed in Ar/H₂/CH₄ microwave discharges during nanocrystalline diamond film synthesis. *Diamond Relat. Mater.*, **15**, 908.
- Al-Qurashi, K., and Boehman, A.L. 2008. Impact of exhaust gas recirculation (EGR) on the oxidative reactivity of diesel engine soot. *Combust. Flame*, **155**, 675.
- Cain, J.P., Gassman, P.L., Wang, H., and Laskin, A. 2010. Micro-FTIR study of soot chemical composition—evidence of aliphatic hydrocarbons on nascent soot surfaces. *Phys. Chem. Chem. Phys.*, **12**, 5206.
- Glassman, I. 1996. *Combustion*, Academic Press, San Diego, California, p. 631.
- Kohse-Höinghaus, K., Oßwald, P., Cool, T.A., Kasper, T., Hansen, N., Qi, F., Westbrook, C.K., and Westmoreland, P.R. 2010. Biofuel combustion chemistry: From ethanol to biodiesel. *Angew. Chem. Int. Ed.*, **49**, 3572.
- Lapuerta, M., Armas, O., Ballesteros, R., and Fernández, J. 2005. Diesel emissions from biofuels derived from Spanish potential vegetable oils. *Fuel*, **84**, 773.
- Lapuerta, M., Armas, O., and Rodríguez-Fernández, J. 2008. Effect of biodiesel fuels on diesel engine emissions. *Prog. Energy Combust. Sci.*, **34**, 198.
- Maricq, M. 2011. Physical and chemical comparison of soot in hydrocarbon and biodiesel fuel diffusion flames: A study of model and commercial fuels. *Combust. Flame*, **158**, 105.
- Santamaría, A., Mondragón, F., Molina, A., Marsh, N.D., Eddings, E.G., and Sarofim, A.F. 2006. FT-IR and ¹H NMR characterization of the products of an ethylene inverse diffusion flame. *Combust. Flame*, **146**, 52.
- Schönborn, A., Ladommatos, N., Williams, J., Allan, R., and Rogerson, J. 2009. The influence of molecular structure of fatty acid monoalkyl esters on diesel combustion. *Combust. Flame*, **156**, 1396.
- Song, J., Alam, M., Boehman, A.L., and Kim, U. 2006. Examination of the oxidation behavior of biodiesel soot. *Combust. Flame*, **146**, 589.
- Szybist, J.P., Song, J., Alam, M., and Boehman, A.L. 2007. Biodiesel combustion, emissions and emission control. *Fuel Process. Technol.*, **88**, 679.
- Vander Wal, R.L., Bryg, V.M., and Hays, M.D. 2010. Fingerprinting soot (towards source identification): Physical structure and chemical composition. *J. Aerosol Sci.*, **41**, 108.
- Zhang, H.R., Eddings, E.G., and Sarofim, A.F. 2008. Pollutant emissions from gasoline combustion. 1. Dependence on fuel structural functionalities. *Environ. Sci. Technol.*, **42**, 5615.
- Zhang, J., He, K., Shi, X., and Zhao, Y. 2011. Comparison of particle emissions from an engine operating on biodiesel and petroleum diesel. *Fuel*, **90**, 2089.
- Zhu, L., Zhang, W., Liu, W., and Huang, Z. 2010. Experimental study on particulate and NO_x emissions of a diesel engine fueled with ultra low sulfur diesel, RME-diesel blends and PME-diesel blends. *Sci. Total Environ.*, **408**, 1050.